Letter

Universal correlations as fingerprints of transverse quantum fluids

Anatoly Kuklov,[1] Lode Pollet,[2,3] Nikolay Prokof'ev,[4] Leo Radzihovsky,[5] and Boris Svistunov[4,6]

[1]*Department of Physics & Astronomy, College of Staten Island and the Graduate Center of CUNY, Staten Island, New York 10314, USA*

[2]*Department of Physics and Arnold Sommerfeld Center for Theoretical Physics, Ludwig-Maximilians-Universität München, Theresienstrasse 37, München D-80333, Germany*

[3]*Munich Center for Quantum Science and Technology (MCQST), Schellingstrasse 4, D-80799 München, Germany*

[4]*Department of Physics, University of Massachusetts, Amherst, Massachusetts 01003, USA*

[5]*Department of Physics and Center for Theory of Quantum Matter, University of Colorado, Boulder, Colorado 80309, USA*

[6]*Wilczek Quantum Center, School of Physics and Astronomy and T. D. Lee Institute, Shanghai Jiao Tong University, Shanghai 200240, China*

(Received 1 November 2023; accepted 5 January 2024; published 23 January 2024)

We study universal off-diagonal correlations in transverse quantum fluids (TQF); a new class of quasi-one-dimensional superfluids featuring long-range-ordered ground states. These exhibit unique self-similar space-time relations scaling with $x^2/D\tau$ that serve as fingerprints of the specific states. The results obtained with the effective field theory are found to be in perfect agreement with *ab initio* simulations of hard-core bosons on a lattice; a simple microscopic realization of TQF. This allows an accurate determination—at nonzero temperature and finite system size—of such key ground-state properties as the condensate and superfluid densities, and characteristic parameter D.

DOI: 10.1103/PhysRevA.109.L011302

Introduction. The concept of a transverse quantum fluid (TQF) originally emerged in the context of superfluid edge dislocations in ^{4}He [1,2] in an attempt to explain the observed "flow-through-solid" phenomena [3–10]. It was subsequently realized [11] that there exists a broad class of quasi-one-dimensional superfluids featuring similar properties. Examples include a superfluid edge of a self-bound droplet of hard-core bosons on a two-dimensional (2D) lattice, a Bloch domain wall in an easy-axis ferromagnet, and a phase separated state of two-component bosonic Mott insulators with the boundary in the counter-superfluid phase (or in a phase of two-component superfluid) on a 2D lattice. The TQF state is a striking demonstration of the conditional character of many dogmas associated with superfluidity and its order parameter field, such as elementary excitations, in general, and the ones obeying the Landau criterion in particular. In sharp contrast with Luttinger liquids—the standard paradigm for 1D quasi-long-ranged superfluids—TQFs feature long-range-ordered ground states supporting persistent currents.

Currently, there are two known classes of TQFs [11]: (i) systems featuring well-defined elementary excitations with a quadratic dispersion, $\omega = Dk^2$, and (ii) so-called *incoherent* TQF systems (iTQFs) where the dynamics of phase fluctuations has diffusive character, $\omega = -iDk^2$, i.e., they lack elementary excitations. All the examples mentioned above belong to the class (i). A minimal iTQF model, most relevant for quantum emulation with ultracold atoms and efficient *ab initio* numeric simulation, is presented in Fig. 1. The Hamiltonian of this hard-core boson system contains only hopping terms between the nearest-neighbor sites with a single 1D path in the x direction (horizontal links at $y = 0$), which forms the iTQF channel. Our analysis equally applies to both geometries shown in the main panel and in the inset.

For computational convenience we focus on systems with particle hole symmetry at half filling and with the same hopping amplitude t between all connected sites. Working in energy units of t and length scales of the lattice spacing, our microscopic model is parameter-free. The ground-state condensate density, n_0, superfluid stiffness, n_s, and the diffusion constant, D, are the key quantities uniquely characterizing the universal iTQF properties of the system.

In this Letter, we show—based on *ab initio* worm algorithm quantum Monte Carlo simulations [12] and predictions of the effective field theory—that finite-size/finite-temperature behavior of the minimal model shown in Fig. 1 [and also that of physically similar but microscopically different model (23)] is perfectly and in full detail described by the iTQF effective field theory. This is so even for relatively small system sizes, L, and with temperatures $T^{-1} \equiv \beta \lesssim L$, providing a powerful tool to clearly reveal the unique off-diagonal correlations—the fingerprint of iTQF—experimentally. Our key results are presented in Figs. 2 and 3.

Effective field theory model: We begin with the iTQF Euclidean low-energy effective action [11] ($\hbar = 1$ throughout)

$$S_{\mathrm{iTQF}} = \frac{1}{2}\sum_{\omega,k}[K_b|\omega| + n_s k^2]|\phi_{\omega,k}|^2, \tag{1}$$

where the parameter K_b, or, equivalently, the diffusion coefficient $D = n_s/K_b$ controls the real-time diffusive dynamics $\omega = -iDk^2$ of the superfluid phase, $\phi(x,\tau)$, for the boson field $\psi \sim e^{i\phi}$.

Neglecting topological defects (instantons), the state with a harmonic action is fully characterized by the Green's function $G(x,\tau) = \langle\psi^*(x,\tau)\psi(0,0)\rangle$, straightforwardly obtained

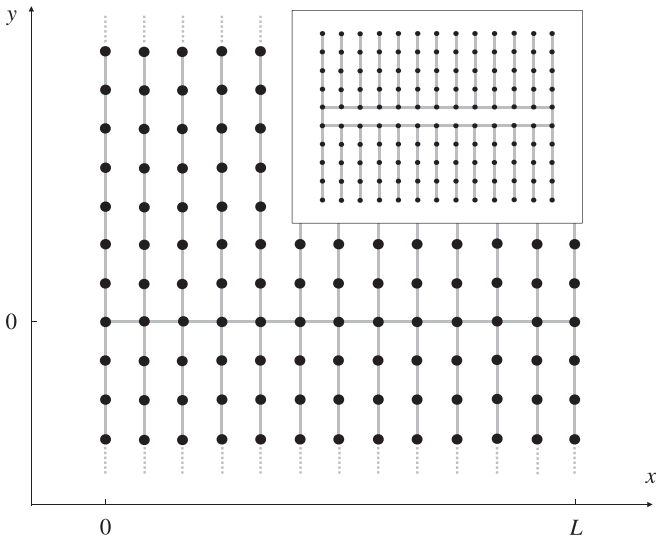

FIG. 1. Minimal iTQF model: Hard-core bosons at filling factor $n = 0.5$ on the square lattice, with all hopping amplitudes between sites in the x direction suppressed, except along the single row at $y = 0$. The nonzero hopping amplitudes are marked by solid lines. Inset: Image of a system of finite length with periodic boundary conditions, supporting a superflow along the central loop, which we expect to be implementable experimentally.

from Gaussian integrals:

$$G(x,\tau) \;=\; n_{\rm uv}\,\Phi(x)\,e^{-\tilde{C}(x,\tau)}, \tag{2}$$

where $n_{\rm uv}$ is the ultraviolet-cutoff-dependent quantity,

$$\Phi(x) = Z^{-1}\sum_{m=-\infty}^{\infty} e^{-\beta E_m}\,e^{i2\pi m x/L}, \tag{3}$$

$$Z = \sum_{m=-\infty}^{\infty} e^{-\beta E_m} \quad \text{with} \quad E_m = \frac{n_s}{2}\frac{(2\pi m)^2}{L}, \tag{4}$$

is the statistical sum of contributions from persistent current states with phase winding numbers m in the system with periodic boundary—otherwise $\Phi(x) = 1$; for details, see Refs. [13,14], and

$$\tilde{C}(x,\tau) \;=\; \frac{1}{2}\,\langle\,[\,\phi(x,\tau)-\phi(0,0)\,]^2\,\rangle, \tag{5}$$

$$\to \int_{k,\omega}[1-\cos(kx+\omega\tau)]\,c(\omega,k). \tag{6}$$

The intergration $\int_{k,\omega} \equiv \int \frac{d\omega dk}{(2\pi)^2}$ is performed with appropriate UV cutoff. The last expression is valid at zero temperature in the thermodynamic limit $L \to \infty$. (There is no need for a τ analog of the Φ factor for TQF because τ windings of the phase are macroscopically expensive.)

The iTQF kernel $c(\omega,k)$ is given by

$$c(\omega,k) \;=\; \frac{D}{n_s}\,\frac{1}{|\omega|+Dk^2} \quad \text{(iTQF)}. \tag{7}$$

Similarly, the TQF state is characterized by $c(\omega,k) = D^2k^2/[n_s(\omega^2+D^2k^4)]$, with $D=\sqrt{n_s/\kappa}$, see Ref. [2]. At zero temperature, both states exhibit off-diagonal long-range order even in 1D, corresponding to a saturation of the integral (6) in the limit of $|\tau|, |x| \to \infty$, leading to a finite condensate fraction n_0 in the superfluid ground state,

$$n_0 = n_{\rm uv}\,e^{-\int_{k,\omega} c(\omega,k)}. \tag{8}$$

This brings us to the UV-cutoff-independent Bogoliubov relation

$$G(x,\tau) \;=\; n_0\;\Phi(x)\,e^{C(x,\tau)},\;\text{for}\;D|\tau|+x^2\to\infty, \tag{9}$$

where $C(x,\tau) \equiv \tilde{C}(\infty,\infty) - \tilde{C}(x,\tau)$.

Simple analysis reveals self-similarity of $C(x,\tau)$ for TQF and iTQF in the thermodynamic limit:

$$C(x,\tau) = \frac{D}{n_s|x|}\,g(D|\tau|/x^2) \tag{10}$$

$$= \frac{\sqrt{D}}{n_s\sqrt{|\tau|}}\,f(|x|/\sqrt{D|\tau|}). \tag{11}$$

Here $g(\sigma)$ and $f(\zeta)$ are dimensionless scaling functions related to each other by the identity $f(\zeta) \equiv g(1/\zeta^2)/\zeta$, $\zeta = 1/\sqrt{\sigma}$. In the TQF case, straightforward integration over ω results in a gaussian integral over k, leading to the transparent final answer:

$$C(x,\tau) = \frac{\sqrt{D}\,e^{-\frac{x^2}{4D|\tau|}}}{4n_s\sqrt{\pi|\tau|}}. \tag{12}$$

For iTQF no-closed form expression for $C(x,\tau)$ can be obtained. Using Ref. [15], one finds

$$g(\sigma) \;=\; \int_{\omega,k}\frac{e^{ik+i\omega\sigma}}{|\omega|+k^2} = \mathrm{Re}\left[\frac{(1+i)e^{\frac{i}{4\sigma}}}{2\sqrt{2\pi\sigma}}\,\mathrm{erfc}\left(\frac{1+i}{2\sqrt{2\sigma}}\right)\right]$$

$$\approx \pi^{-1}(1-12\sigma^2+\ldots), \quad \text{for} \quad \sigma \ll 1. \tag{13}$$

In a complementary limit,

$$f(\zeta) \approx \frac{1}{2\sqrt{2\pi}}(1-\zeta^2/4+\ldots), \quad \text{for} \quad \zeta \ll 1. \tag{14}$$

In a system of a finite length L and a finite temperature T, these relations can be used as long as $|x| \ll L$ and $|\tau| \ll \beta$. Otherwise, the finite-temperature and finite-size effects become significant and thus need to be accurately addressed.

Finite temperature and system size. For a finite system of length L with periodic boundary conditions and at a low but nonzero temperature, the correlator $C(x,\tau)$ in Eq. (9) is given by (measuring x and τ in units of $L/2$ and $\beta/2$, respectively, in all expressions)

$$C(x,\tau) = C_0 + \sum_{\substack{m,\,n=-\infty\\(|m|+|n|\neq 0)}}^{\infty} e^{i\pi n x}e^{i\pi m\tau}c_{mn}, \tag{15}$$

where $c_{mn} \equiv c(\omega_m,k_n)/(\beta L)$, $\omega_m = 2\pi m/\beta$, $k_n = 2\pi n/L$, and

$$C_0 = \int_{\omega,k} c(\omega,k) \;-\; \sum_{\substack{m,\,n\\(|m|+|n|\neq 0)}} c_{mn}. \tag{16}$$

Here, both the integral and the sum have ultraviolet frequency and momentum cutoffs, which mutually cancel. The constant C_0 originates from our convention that n_0 in Eq. (9) be exactly equal to the ground-state condensate density in an infinitely

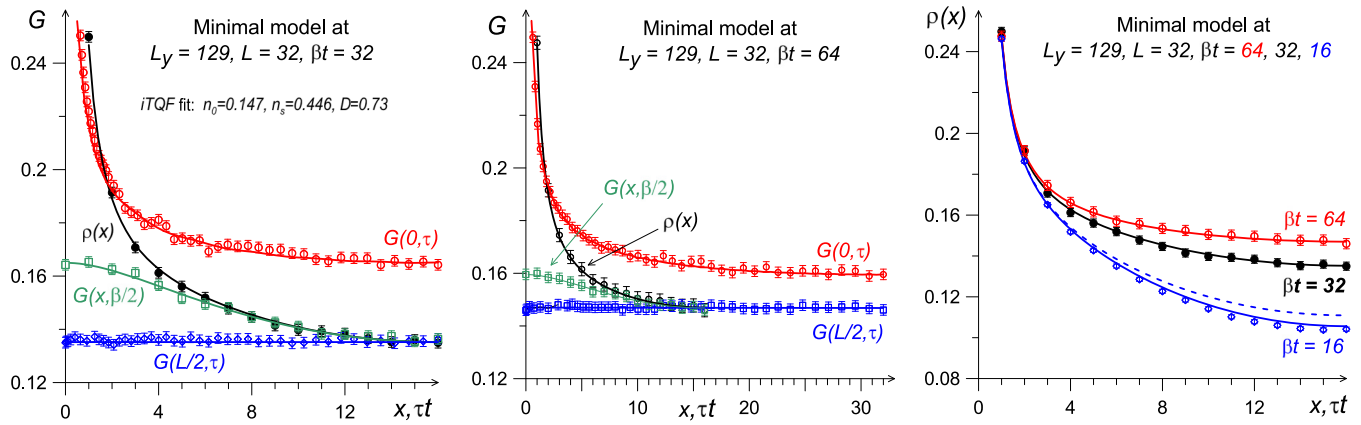

FIG. 2. Left panel: Single-particle Green's function $G(x,\tau)$ of the minimal model (Fig. 1) along four representative space-time directions for $\beta t = 32$. Solid lines are fits to the predictions of the effective iTQF theory using n_0 and D as the only fitting parameters ($n_s = 0.446$ is computed from statistics of winding number fluctuations). The $G(0,0) = 0.5$ point is excluded to focus on the universal low-energy behavior. Central panel: Green's function for $\beta t = 64$ with solid lines representing fit-free predictions of the effective iTQF theory using parameters determined for $\beta t = 32$. Right panel: Density matrix $\rho(x)$ for three different temperatures. Solid lines are theoretical predictions using parameters determined for $\beta t = 32$. In numeric simulations, temperatures are known and the superfluid stiffness n_s is computed, which leaves only two fitting parameters, n_0 and D, to describe all three curves. In the experiment, where not only n_s but also temperatures may not be known, fitting the curves involves six parameters. An accurate fit thereby provides not only quantitative evidence for iTQF state and its ground state properties, but also a protocol for determining the three temperatures at which $\rho(x)$ were measured. The dashed line for $\beta t = 16$ shows how the fit fails when only the state with zero phase winding is taken into account, i.e., when $\Phi = 1$.

large system. [The $m = n = 0$ component is absorbed in the definition of condensate; this will be implied in what follows.]

In the iTQF case, we have

$$c_{mn} = \frac{L/\beta}{4\pi^2 n_s}\frac{1}{n^2 + \frac{\gamma^2|m|}{\pi^2}}, \quad \gamma = \sqrt{\frac{\pi}{2}}\frac{L}{\sqrt{D\beta}} \quad \text{(iTQF)}.$$

Performing standard summation over n, we obtain

$$C(x,\tau) = \frac{L/\beta}{2n_s}\left[\frac{x(x-2)}{4} + \frac{\lambda_0 + \lambda_1(x,\tau)}{\gamma}\right], \tag{17}$$

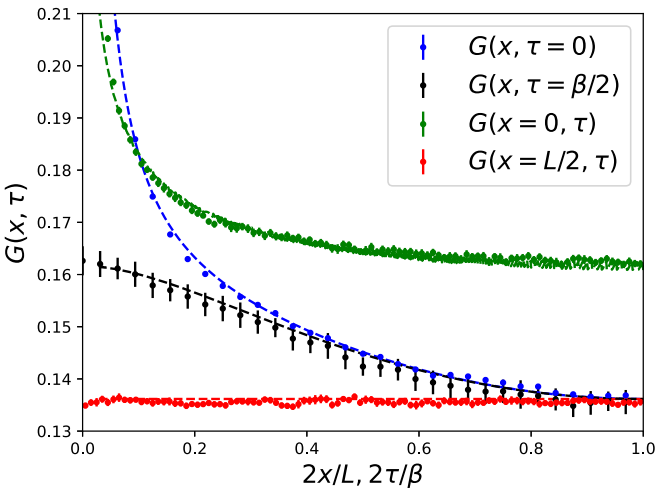

FIG. 3. Green's functions for the model Eq. (23). The dashed lines are the fits by the iTQF theory. The fit parameters have been optimized for $G(x,\tau = 0)$ and are then reused for the other cases. The superfluid stiffness $n_s = 0.5279(4)$ is obtained from the fluctuations in winding numbers along the x axis, $n_s = (L/\beta)\langle W_x^2\rangle$. The fit results are $n_0 = 0.1481(4)$ and $\gamma = 8.86(9)$ (or $D \approx 1.28$).

where

$$\lambda_1(x,\tau) = \sum_{m=1}^{\infty}\frac{\cos(\pi m\tau)}{\sqrt{m}}\frac{\cosh(|1-x|\gamma\sqrt{m})}{\sinh(\gamma\sqrt{m})}, \tag{18}$$

$$\lambda_0 = c_0 - \sum_{m=1}^{\infty}\frac{1}{\sqrt{m}}[\coth(\gamma\sqrt{m}) - 1], \tag{19}$$

$$c_0 = \lim_{m_*\to\infty}\left[2\sqrt{m_* + 1/2} - \sum_{m=1}^{m_*}\frac{1}{\sqrt{m}}\right] \approx 1.460. \tag{20}$$

(The term $1/2$ under the square root dramatically enhances the convergence.)

Of particular experimental interest is the single-particle density matrix $\rho(x) = G(x,0)$ at nonzero temperature and finite system size given by

$$\rho(x) = n_0\Phi(x)\exp\left\{-\frac{Lx(2-x)}{8n_s\beta} + \frac{\sqrt{D}\,[c_0 + \lambda_\rho(x)]}{n_s\sqrt{2\pi\beta}}\right\}, \tag{21}$$

$$\lambda_\rho(x) = \sum_{m=1}^{\infty}\frac{1}{\sqrt{m}}\left[1 - \frac{\cosh(\gamma\sqrt{m}) - \cosh(|1-x|\gamma\sqrt{m})}{\sinh(\gamma\sqrt{m})}\right]. \tag{22}$$

The dependence of ρ on β and L cannot be reduced to a single scaling combination of these parameters, meaning that both can be used independently for probing and verifying the universal off-diagonal correlations. The divergence of $\lambda_1(x,\tau)$ and $\lambda_\rho(x)$ at $x,\tau \to 0$ signals their sensitivity to UV cutoff [formally taken to infinity in Eqs. (18) and (22)]; this divergence is eliminated inside $\tilde{C}(x,\tau)$ by the UV-cutoff-dependent condensate density, as is clear from Eq. (5).

In Fig. 2, we show the result of worm-algorithm quantum Monte Carlo simulations [12] of the minimal model with

relatively large system size L_y in the y direction, but smaller length L in the iTQF direction (with both lengths measured in units of the lattice spacing). The temperature $T \sim L^{-1} \gg t/L^2$ should be considered high given that the low-frequency iTQF dynamics is characterized by $\omega \sim Dk^2$. The choice of L_y in our simulations corresponds to the thermodynamic limit, that is, $L_y \gg \beta t$. Since n_s is computed with high accuracy from statistics of path-integral winding number fluctuations, two parameters, n_0 and D, describe all Green's function data in the space-time domain. Clearly, n_0 is responsible only for the overall signal amplitude at large x and τ. Thus D is solely responsible for the shape of the curves. Apart from providing perfect description of all data in the asymptotic limit, the theory works remarkably well down to the lattice constant distance and $\tau t \lesssim 1$, see left panel in Fig. 2.

The central panel in Fig. 2 demonstrates that non-zero temperature effects are under precise theoretical control. In this case, simulation data for lower temperature (larger β) are reproduced by simply taking parameters deduced from the higher temperature fits. The right panel in Fig. 2 is more relevant to the possible experimental observation of the iTQF state: while it is relatively standard to recover the density matrix from the measured momentum distribution, there is no easy direct access to the Green's function in imaginary time. However, if several density matrices at different temperatures are measured, their joint fit will provide access not only to the iTQF ground state parameters, but also constitute an accurate thermometry protocol. Moreover, the difference between the solid and dashed lines for the $\beta t = 16$ case indicates that the density matrix data at elevated temperature are sensitive enough to resolve the persistent currents contribution and, in particular, can be used to estimate n_s directly from $\Phi(x) - 1 \approx -2e^{-\beta E_1}[1 - \cos(2\pi x/L)]$.

In order to further show the universality of the theory, we have also simulated the microscopic model of Ref. [16],

$$H = -\sum_i a_i^\dagger a_{i+1} - \sum_{i,j} b_{i,j}^\dagger b_{i,j+1} - t_\perp \sum_i a_i^\dagger b_{i,0} + \text{H.c.}, \tag{23}$$

where the a_i bosons are moving along the x axis as in Fig. 1, and the b bosons, along the y axis, with the hopping amplitude $t_\perp$ between the a and b bosons. Despite microscopic differences from the model in Fig. 1, model (23) exhibits the same low-energy universal iTQF phenomenology. We have demonstrated this for the system with $L = \beta = 64$, $L_y = 128$, and $t_\perp = 1$. The correlation functions and the corresponding fits are presented in Fig. 3: Although the fit has been performed for the equal time single-particle density matrix, the two fit parameters fully specify the other Green functions as well [17].

Summary and conclusion. Motivated by a number of recently proposed physical realizations, we demonstrated how an effective field theory can be used to make detailed predictions for space-time correlations for finite-size systems at nonzero-temperatures for two types of transverse quantum fluids, which constitute a new class of quasi-one-dimensional quantum fluids that even in 1D exhibit an off-diagonal (superfluid) long-range-ordered ground states. Perfect agreement with quantum Monte Carlo simulations allows us to state that all effective field theory parameters, and even system temperature, can be reliably extracted from the one-particle density matrix measurements in finite-size systems, e.g.. in cold-atom-engineered TQFs. We propose that such benchmarking experiments be used for measuring other TQF properties such as real-time dynamics, entanglement, out-of-time-order correlators, full-counting distribution functions, to name a few, because computing them is difficult or even impossible by existing analytical treatments or numerical simulations.

Acknowledgments. The research of L. R. was supported by the Simons Investigator Award from the Simons Foundation. L.R. thanks The Kavli Institute for Theoretical Physics for hospitality while this manuscript was in preparation, during Quantum Crystals and Quantum Magnetism workshops, and support from the National Science Foundation under Grants No. NSF PHY-1748958 and No. PHY-2309135. L.P. acknowledges funding by the Deutsche Forschungsgemeinschaft (DFG, German Research Foundation) under Germany's Excellence Strategy – EXC-2111 – 390814868. A.K., B.S., and N.P. acknowledge support from the National Science Foundation under Grants No. DMR-2032136 and No. DMR-2032077. Some of the quantum Monte Carlo codes [18] make use of the ALPSCore libraries [19,20].

[1] A. B. Kuklov, L. Pollet, N. V. Prokof'ev, and B. V. Svistunov, Phys. Rev. Lett. **128**, 255301 (2022).
[2] L. Radzihovsky, A. Kuklov, N. Prokof'ev, and B. Svistunov, Phys. Rev. Lett. **131**, 196001 (2023).
[3] M. W. Ray and R. B. Hallock, Phys. Rev. Lett. **100**, 235301 (2008); Phys. Rev. B **79**, 224302 (2009); **81**, 214523 (2010).
[4] Ye. Vekhov and R. B. Hallock, Phys. Rev. Lett. **109**, 045303 (2012).
[5] R. B. Hallock, J. Low Temp. Phys. **197**, 167 (2019).
[6] Z. G. Cheng, J. Beamish, A. D. Fefferman, F. Souris, S. Balibar, and V. Dauvois, Phys. Rev. Lett. **114**, 165301 (2015); Z. G. Cheng and J. Beamish, *ibid.* **117**, 025301 (2016).
[7] J. Shin, D. Y. Kim, A. Haziot, and M. H. W. Chan, Phys. Rev. Lett. **118**, 235301 (2017).
[8] J. Shin and M. H. W. Chan, Phys. Rev. B **99**, 140502(R) (2019).
[9] J. Shin and M. H. W. Chan, Phys. Rev. B **101**, 014507 (2020).
[10] M. H. W. Chan, J. Low Temp. Phys. **205**, 235 (2021).
[11] A. Kuklov, N. Prokof'ev, L. Radzihovsky, and B. Svistunov, arXiv:2309.02501.
[12] N. V. Prokof'ev, B. V. Svistunov, and I. S. Tupitsyn, Zh. Eksp. Teor. Fiz. **114**, 570 (1998); Sov. Phys. JETP **87**, 310 (1998).
[13] N. V. Prokof'ev and B. V. Svistunov, Phys. Rev. B **61**, 11282 (2000).
[14] B. Svistunov, E. Babaev, and N. Prokof'ev, *Superfluid States of Matter* (Taylor & Francis, London, 2015).
[15] *Handbook of Mathematical Functions*, edited by M. Abramowitz and I. Stegun (Dover, New York, 1972).
[16] Z. Yan, L. Pollet, J. Lou, X. Wang, Y. Chen, and Z. Cai, Phys. Rev. B **97**, 035148 (2018).
[17] These results supersede the analysis of Ref. [16]; see also Z. Yan, L. Pollet, J. Lou, X. Wang, Y. Chen, and Z. Cai, Phys. Rev. B **108**, 199905(E) (2023).
[18] N. Sadoune and L. Pollet, Scipost Phys. Codebases 9 (2022).
[19] A. Gaenko *et al.*, Comput. Phys. Commun. **213**, 235 (2017).
[20] M. Wallerberger *et al.*, arXiv:1811.08331 (2018).